Self-assembled Monolayers of 1,4-Benzenedimethanethiol on Polycrystalline Silver and Gold Films: An Investigation of Structure, Stability, Dynamics, and Reactivity

K. V. G. K. Murty, M. Venkataramanan, and T. Pradeep*

Department of Chemistry and Regional Sophisticated Instrumentation Centre, Indian Institute of Technology, Madras 600 036, India

Received March 2, 1998. In Final Form: May 28, 1998

1,4-Benzenedimethanethiol ($HS-CH_2-C_6H_4-CH_2-SH$, BDMT) adsorbs dissociatively on silver and gold surfaces yielding self-assembled monolayers with the thiolate structure. Whereas the molecule adsorbs flat on silver as a result of the loss of two thiol protons, it adsorbs with the molecular plane perpendicular to the gold surface with the loss of one thiol proton. This is manifested by the presence of the ring C−H and S−H stretches and the S−C−H bend for the Au monolayer and the absence of these for the Ag monolayer in the surface-enhanced Raman spectra. The difference in adsorbate geometry is presumably due to the changes in interaction and not to differences in the lattice constants of the two surfaces, which is rather small. In both cases, metal−adsorbate π bonding is weak, resulting in only small shifts in the ring modes. BDMT monolayers are more stable than alkanethiol monolayers and desorb only at a fairly high temperature of 423 K in air, whereas alkanethiols desorb below 373 K. An increase in temperature leads to structural changes in the Au monolayer and the molecules begin to lie flat on the surface, and desorption occurs from this state. The Ag monolayer is less stable thermally and desorption is eventless. Difference in the desorption temperatures point to the importance of energetics of self-assembly in determining the stability. The thiol proton on gold surfaces can be removed easily by exposing the monolayer to basic solutions. The gold monolayer upon exposure to thiols leads to the formation of disulfides, suggesting the formation of a prototypical bilayer. A completely new S−S stretching frequency is seen upon reaction with 4-methoxybenzenethiol (MOBT) with the complete absence of the S−H stretch. Other spectral features of the bilayer can be attributed to BDMT and MOBT subunits. The respective thiols in solution, however, do not react, leading to disulfide. Reaction with silver monolayer leads to the displacement of BDMT for MOBT and no reaction is observed. With *n*-alkanethiols, the reactivity decreases with the alkane chain length. The alkanethiol part of the spectrum resembles that of the corresponding self-assembled monolayer. Surface-enhanced reactivity of the type observed here has not been reported hitherto. The MOBT part of the bilayer desorbs first after cleaving the S−S bond and BDMT leaves the surface subsequently. X-ray exposure of the monolayers leads to beam-induced damage which is manifested in the Raman spectra. Whereas the damage is severe for Ag, part of the Au monolayer survives X-ray exposure.

Introduction

One of the principal needs of research in self-assembled monolayers (SAMs) is to have sufficiently sensitive tools for their characterization. Surface spectroscopies of various kinds and techniques of electrochemistry have been by far the most important tools for SAM research.[1] Surface-enhanced Raman scattering (SERS)[2] has been used extensively, primarily because of the surface selection rules,[3] which help in understanding the orientation of the surface species. In the case of surface infrared spectroscopy, the selection rules are rather simple;[4] they permit the observation of modes whose transition dipole moments have components perpendicular to the surface. In SERS, the selection rules are more complex, which enhance vibrations parallel as well as perpendicular to the surface.[5] Despite this complexity, for a number of aromatics, adsorbate orientation has been deduced from SERS measurements.[6] This has been principally based on the analysis of aromatic C−H vibrations and the relative enhancement of in-plane with respect to out-of-plane ring modes when the adsorbate becomes perpendicular to a planar surface geometry, although the cause of enhancement of certain peaks is not clearly understood.[6a] Because of these effects and the significant downshift of the ring breathing modes due to the ring-surface π-orbital overlap, the flat orientation of some organics on gold[6a,e] and silver[6b,h] surfaces has now been conclusively established. Along

* To whom all correspondence should be addressed.

(1) Ulman, A. *An Introduction to Ultrathin Organic Films from Langmuir−Blodgett to Self-assembly*; Academic Press: New York, 1991.

(2) (a) Otto, A.; Mrozek, I.; Grabhorn, H.; Akemann, W. *J. Phys. Condensed Matter Phys.* **1992**, *4*, 1143−1212. (b) Moskovits, M. *Rev. Mod. Phys.* **1985**, *57*, 783−826. (c) Otta, O. *J. Raman Spectrosc.* **1991**, *22*, 743−752. (d) Suetaka, W. *Surface Infrared and Raman Spectroscopy*; Plenum Press: New York, 1995. (e) Chang, R. K., Furtak, T. E., Eds.; *Surface Enhanced Raman Scattering*; Plenum Press: New York, 1982.

(3) Moskovits, M. *J. Chem. Phys.* **1982**, *77*, 4408−4416.

(4) For a latest report, see Johnson, E.; Aroca, R. *J. Phys. Chem.* **1995**, *99*, 9325−9330.

(5) See, for example, Bryant, M. A.; Pemberton, J. E. *J. Am. Chem. Soc.* **1991**, *113*, 8284−8292.

(6) (a) Geo, X.; Davies, J. P.; Weaver, M. J. *J. Phys. Chem.* **1990**, *94*, 6858−6864. (b) Lee, T. G.; Kim, K.; Kim, M. S. *J. Raman Spectrosc.* **1991**, *22*, 339−344. (c) Bryant, M. A.; Pemberton, J. E. *J. Am. Chem. Soc.* **1991**, *113*, 3629−3637. (d) Gao, P.; Weaver, M. J. *J. Phys. Chem.* **1989**, *93*, 6205−6211. (e) Gao, P.; Weaver, M. J. *J. Phys. Chem.* **1985**, *89*, 5040−5046. (f) Creighton, J. A. *Surf. Sci.* **1983**, *124*, 209−219. (g) Joo, T. H.; Kim, K.; Kim, M. S. *J. Mol. Struct.* **1987**, *158*, 265−274. (h) Cho, S. H.; Han, H. S.; Jang, D.-J.; Kim, K.; Kim, M. S. *J. Phys. Chem.* **1995**, *99*, 10594−10599. (i) Kwon, C. K.; Kim, M. S.; Kim, K. *J. Raman Spectrosc.* **1989**, *20*, 575−580. (j) Kwon, C. K.; Kim, M. S.; Kim, K. *J. Mol. Struct.* **1987**, *162*, 201−210. (k) Joo, T. H.; Kim, M. S.; Kim, K. *J. Mol. Struct.* **1987**, *160*, 81−89. (l) Joo, T. H.; Kim, K.; Kim, H.; Kim, M. S. *Chem. Phys. Lett.* **1985**, *117*, 518−522. (m) Suh, J. S.; Moskovits, M. *J. Am. Chem. Soc.* **1986**, *108*, 4711−4718. (n) Joo, T. H.; Kim, K.; Kim, M. S. *J. Phys. Chem.* **1986**, *90*, 5816−5819. (o) Clavijo, R. E.; Mutus, B.; Aroca, R.; Dimmock, J. R.; Phillips, O. A. *J. Raman Spectrosc.* **1988**, *19*, 541−546. (p) Lee, S. B.; Kim, K.; Kim, M. S. *J. Raman Spectrosc.* **1991**, *22*, 811−817. (q) Lee, T. G.; Kim, K.; Kim, M. S. *J. Phys. Chem.* **1991**, *95*, 9950−9955.

S0743-7463(98)00249-2 CCC: $15.00
Published on Web 08/21/1998

with atmospheric pressure measurements, ultrahigh vacuum studies[6a] have also been done in this regard.

By virtue of the specific orientation of species at the surface, there is a possibility that certain reactions can occur more easily on SAMs than in the solution.[7] It is also likely that there can be surface activation of a reaction. This methodology of reaction at SAM surfaces can lead to modified monolayers with appropriate functionalities which can be interesting from the point-of-view of applications. The same methodology can be used to make oriented molecules at molecular surfaces, leading to self-assembled multilayers. Formation of such multilayers can be used to probe important aspects of surface-enhancement processes. The difficulty, of course, is the characterization of such modified monolayers.

There are several ways of effecting transformation at molecular surfaces, and the methods range from simple exposure of reagents to ion beam collisions.[8] A methodology by which only the top functionality is modified is important from the point-of-view of site-specific properties.[7] We have been working along these lines in the recent past,[8e,f] and during the course of this investigation, it became clear to us that the best method for studying modifications in the molecular scale is SERS. By applying our new methodology[9] to make surface-enhanced Raman-active films, we have found that the preparation of SAMs on SERS-active surfaces has become extremely simple and reliable. This made this investigation feasible.

Adsorbate geometry has been one of the subjects of detailed experimental and theoretical investigation in monolayer research. For alkane thiols on gold, the preferred adsorption site is the 3-fold hollow site leading to a $(\sqrt{3} \times \sqrt{3})$R 30° adlayer of sulfur atoms.[10] There are reports on disulfide formation at the surface[11] and the presence of different types of sulfur atoms.[12] However, most of the reports point to the thiolate (RS^-) structure at the surface.[13] Detailed structural studies by scanning probe microscopies[14] and rare gas atom scattering[15] have been confined to alkanethiol monolayers only. Probability of different adsorption sites exists in other monolayers.

There are only a few reports on the thermal stability of monolayers; here again data mostly pertain to alkanethiol systems. On the contrary, thermal behavior of Langmuir−Blodgett monolayers and multilayers have been investigated in detail.[16] Infrared spectroscopy has been used to understand the phase stability of long-chain alkanethiol monolayers.[17] No temperature-dependent Raman study of monolayers has come to our attention. Dynamics of small molecules at surfaces with a change in temperature in the context of surface science has been a rather active area using a number of tools such as high-resolution electron energy loss spectroscopy (HREELS).[18]

Monolayer reactivity has also not been examined in detail. The reference here pertains to stable monolayers, not adsorbed model systems in vacuum, which have been studied in detail by surface scientists. Electron-transfer processes[19] have been investigated with monolayers in solution, but the emphasis has not been the chemical changes of the monolayers. Chemical transformations in monolayers induced by photons have been studied, which have impications in technology.[20] To prepare organic multilayers by self-assembly, terminal functionalities of the monolayers have been transformed chemically; an example is the conversion of an ester-terminated surface to a hydroxyl-terminated one.[21] There are other reports on multilayer formation as well.

In the following, we shall present a study of the monolayers of 1,4-benzenedimethanethiol (BDMT) on gold and silver films using surface-enhanced Raman scattering. In addition, we have used X-ray photoelectron spectroscopy for the characterization of monolayers. The molecule adsorbs dissociatively on both the surfaces. On gold, the adsorption geometry is perpendicular to the surface with one S−H projecting at the surface. On silver, both the thiol protons are lost and the benzene ring lies flat. In both cases, the π-interaction between the ring and the surface is not strong, resulting in only small frequency downshifts for the ring modes. The monolayers are stable up to a temperature of 423 K. Whereas the desorption happens directly on silver, the monolayer tends to lie flat on gold upon heating and thereafter desorbs. The dynamics of assembled molecules appears to be an interesting phenomena. A thiol-terminated monolayer upon exposure to 4-methoxybenzenethiol results in the formation of a disulfide, and the resulting SAM can be characterized as a prototypical multilayer. The reactivity decreases with the chain length in *n*-alkanethiols and in octadecanethiol; the disulfide formation is almost undetectable. Such a reaction is absent on the silver surface. A temperature-dependent study revealed that the modified monolayer is as stable as the original one, the thermal stability of which is higher than that of the alkanethiol SAMs.[22] Surface-enhanced reactivity of the kind reported here leading to organic multilayers has not been reported

(7) Some of the critical issues in SAM research are discussed in Whitesides, G. M.; Frguson, G. S.; Allara, D. L.; Scherson, D.; Speaker, L.; Ulman, A. *Surf. Chem.* **1993**, *3*, 49.

(8) (a) See for an account of various low-energy ion-induced processes Cooks, R. G.; Ast, T.; Pradeep, T.; Wysocki, V. A. *Acc. Chem. Res.* **1994**, *27*, 316−323. (b) Cooks, R. G.; Ast, T.; Mabud, A., MD. *Int. J. Mass Spectrom. Ion Processes* **1990**, *100*, 209−265. (c) Pradeep, T.; Riederer, D. E.; Ast, T.; Cooks, R. G. *Rapid Commun. Mass Spectrometry* **1993**, *7*, 711−713. (d) Miller, S. A.; Luo, H.; Pachuta, S. J.; Cooks, R. G. *Science* **1997**, *275*, 1447−1450. (e) Bindu, V.; Dorothy, A.; Pradeep, T. *Int. J. Mass Spectrom. Ion Processes* **1996**, *155*, 69−78. (f) Bindu, V.; Venkataramanan, M.; Pradeep, T. *Mol. Phys.*, communicated.

(9) Sandhyarani, N.; Murty, K. V. G. K.; Pradeep, T. *J. Raman. Spectrosc.*, in press.

(10) Sellers, H.; Ulman, A.; Shnidman, Y.; Eilers, J. E. *J. Am. Chem. Soc.* **1993**, *115*, 9389−9401 and references therein.

(11) Fenter, P.; Eberhardt, A.; Eisenberger, P. *Science* **1994**, *266*, 1216−1218.

(12) Zubragel, Ch.; Deuper, C.; Schneider, F.; Neumann, M.; Grunze, M.; Schertal, A.; Woll, Ch. *Chem. Phys. Lett.* **1995**, *238*, 308−312.

(13) (a) Nuzzo, R. G.; Dubois, L. H.; Allara, D. V. *J. Am. Chem. Soc.* **1990**, *112*, 558−569. (b) Whitesides, G. M.; Laibinis, P. E. *Langmuir* **1990**, *6*, 87−95. (c) Laibinis, P. E.; Nuzzo, R. G.; Whitesides, G. M. *J. Phys. Chem.* **1992**, *96*, 5097−5105. (d) Nuzzo, R. G.; Zegarski, B. R.; Dubois, L. H. *J. Am. Chem. Soc.* **1987**, *109*, 733−740.

(14) (a) McDermott, C. A.; McDermott, M. T.; Green, J. B.; Porter, M. D. *J. Phys. Chem.* **1995**, *99*, 13257−13267. (b) Widrig, C. A.; Alves, C. A.; Porter, M. D. *J. Am. Chem. Soc.* **1991**, *113*, 2805−2810. (c) Alves, C. A.; Smith, E. L.; Porter, M. D. *J. Am. Chem. Soc.* **1992**, *114*, 1222−1227.

(15) (a) Chidsey, C. E. D.; Liu, G.-Y.; Rowntree, P.; Scoles, G. *J. Chem. Phys.* **1989**, *91*, 4421−4423. (b) Camillone, N.; Chidsey, C. E. D.; Liu, G.-Y.; Putvinski, T. M.; Scoles, G. *J. Chem. Phys.* **1991**, *94*, 8493−8502.

(16) (a) Rabe, J. P.; Swalen, J. D.; Rabolt, J. F. *J. Chem. Phys.* **1987**, *86*, 1601−1607. (b) Rothberg, L.; Higashi, G. S.; Allara, D. L.; Garoff, S. *Chem. Phys. Lett.* **1987**, *133*, 67−71. (c) Richardson, W.; Blasie, J. K. *Phys. Rev. B* **1989**, *39*, 12165−12181.

(17) Nuzzo, R. G.; Korenic, M.; Dubois, L. H. *J. Chem. Phys.* **1990**, *93*, 767−773.

(18) See, for example, Ibach, H.; Mills, D. L. *Electron Energy Loss Spectroscopy and Surface Vibrations*; Academic Press: New York, 1982.

(19) (a) Campbell, D. J.; Herr, B. R.; Hulteen, J. C.; Van Duyne, R. P.; Mirkin, C. A. *J. Am. Chem. Soc.* **1996**, *118*, 10211−10219. (b) Smalley, J. F.; Feldberg, S. W.; Chidsey, C. E. D.; Linford, M. R.; Newton, M. D.; Liu, Y.-P. *J. Phys. Chem.* **1995**, *99*, 13141−13149. (c) Carter, M. T.; Rowe, G. K.; Richardson, J. N.; Tender, L. M.; Terrill, R. H.; Murray, R. W. *J. Am. Chem. Soc.* **1995**, *117*, 2896−2899. (d) Forster, R. J.; Faulkner, L. R. *J. Am. Chem. Soc.* **1994**, *116*, 5453−5461.

(20) (a) Yang, X. M.; Tryk, D. A.; Hasimoto, K.; Fujishima, A. *Appl. Phys. Lett.* **1996**, *69*, 4020−4022. (b) Kang, D.; Wrighton, M. S. *Langmuir* **1991**, *7*, 2169−2174.

(21) Tillman, N.; Ulman, A.; Penner, T. L. *Langmuir* **1989**, *5*, 101−111.

(22) Sandhyarani, N.; Pradeep, T. *Vacuum*, in press.

hitherto. The results presented here extend the scope of SAM research and suggest a potential method for the synthesis of functional molecular surfaces. The XPS studies give clear evidence for X-ray-induced damage which has been confirmed by subsequent SERS measurements.

Experimental Section

Preparation of Raman-active gold and silver films have been discussed in detail before.[9] Briefly, an oxidized aluminum foil of 20-μm thickness made by heating it in air at 873 K for 5 h is sputter-coated with about 2000 Å of gold or silver in an Edwards sputter coater. The gold and silver used for coating were of 99.9% purity. The films prepared this way have been shown to be excellent substrates for SERS work.[9] The films show corrugations in the submicrometer scale in scanning electron microscopy. All SERS measurements on these surfaces have given excellent spectra, the intensities of which are reproducible from batch to batch under identical conditions.

Monolayers were prepared following standard literature procedure used for the preparation of alkanethiol SAMs.[1] Chemicals used for this work were purchased from Aldrich Chemical Co. All the thiol solutions were prepared in absolute ethanol, and the films were exposed to these solutions overnight. The films were kept in the vacuum chamber of the sputter coater prior to immersion in the solution. No washing was done prior to immersion. The films were removed from the solution, washed with absolute ethanol repeatedly, and air-dried prior to measurements. The surfaces appeared the same to the naked eye after the monolayer formation. To make pH-dependent measurements, the films were exposed to aqueous thiol solutions prepared with NaOH or HCl or the prepared monolayers were immersed in acidic or alkaline solutions for 2 h. The monolayers were washed with water prior to analysis. To effect modifications, the BDMT monolayers prepared this way were exposed to 1 mM solutions of the appropriate thiol in ethanol overnight. Washing was done as in the case of the BDMT monolayers.

Raman spectra were recorded with a Bruker IFS66v FT-IR spectrometer with a FT-Raman accessory. An Nd:YAG laser (1064 nm) was used as the excitation source. All the spectra were recorded with 500 scans. Each spectrum took about 1 h for acquisition. The laser power was kept at 70 mW and the beam diameter was 2 μm. Variable temperature measurements in the range of 298−493 K were performed with a home-built heater with a programmable temperature controller. At each temperature, the sample was kept for at least 20 min for stabilization before the measurement. The sample compartment in the spectrometer was kept at atmosphere.

X-ray photoelectron spectra were recorded with a VG ESCALAB MkII spectrometer using unmonochromatized MgKα radiation as the excitation source. The binding energies are referenced to the Au $4f_{7/2}$ peak at 84.0 eV. The samples were introduced into the spectrometer immediately after being washed in alcohol. The monolayers showed no effect of charging during the measurements. No desorption was noticed during measurement. The electron flux of the X-ray gun was kept at 70 mW to keep the beam-induced damage low. Due to poor signal intensity, each spectrum was an average of 20 measurements of 2 min duration. The spectra were acquired in the constant analyzer energy mode. A pass energy of 50 V was used for the C, O, Au, and Ag regions and a pass energy of 100 V was used for the S 2p region.

Ab initio molecular orbital (MO) calculations were performed using the Gaussian 94w program[23] with the 6-31G* basis set.[24]

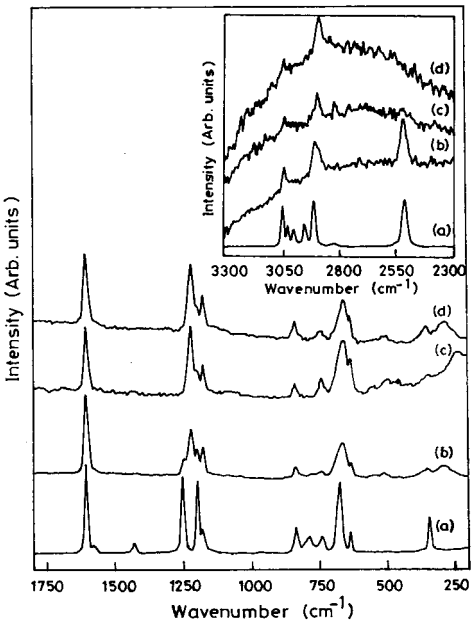

Figure 1. (a) The ordinary Raman (OR) spectrum of BDMT solid and the SER spectra of BDMT monolayers on (b) Au, (c) Ag, and (d) Au monolayer exposed to NaOH solution. The expanded C−H stretching region of Au and Ag monolayers are given in the inset in the same sequence.

All the molecular parameters in the C_s symmetry were optimized, and the optimized parameters were used for the final frequency calculation. Calculations were also done on the singlet and triplet dithiolate ion in the C_s point group. Calculations were done on a Pentium workstation.

Scanning electron micrographs were taken with a JEOL SEM.

Results and Discussion

Structure. Figure 1 shows the ordinary Raman (OR) spectrum of BDMT and the surface-enhanced Raman spectra of the monolayers on gold and silver. The spectra are assigned as in Table 1. To perform the assignments, ab initio MO calculations were performed in the HF/6-31G* level on the BDMT molecule as well as the dianion in its singlet and triplet states. The molecular parameters were fully optimized in the C_s symmetry before the Raman spectrum was computed. The optimized molecular structures of the thiol and the dithiolate anion are shown in Figure 2. The significant molecular parameters obtained are also shown in the figure. Molecular parameters of the singlet dithiolate anion are larger than those of the thiol. In the triplet state, the geometry is similar to that of the singlet except that the benzene-ring−CH_2 bond length is significantly reduced. The frequencies computed for the singlet state are in agreement with those of the experiment and are listed in Table 1.

The spectra of the monolayers resemble the OR spectrum of the solid. All of the bands are red-shifted upon adsorption. Compared to the Au monolayer, the Ag monolayer has fewer peaks. This is especially clear in the C−H region (see the inset) where the S−H stretch is completely absent in Ag. BDMT has been the subject of an earlier SERS study by Kim et al. who studied its adsorption on a silver sol.[6q] The essential conclusion of the study was that the molecule dissociatively chemisorbs on silver with the molecular plane flat on the metal surface. On Au, only one thiol proton is lost and the other S−H stretch is still seen in the spectrum (Figure 1b). The S−Au chemisorption is manifested in the frequency downshift of the C−S mode in both Au and Ag. The extent of shift ($\sim$10 cm^{-1}) is comparable to alkanethiolates on Au[5] and

(23) Frisch, M. J.; Trucks, G. W.; Schlegel, H. B.; Gill, P. M. W.; Johnson, B. G.; Robb, M. A.; Cheeseman, J. R.; Keith, T. A.; Petersson, G. A.; Montgomery, J. A.; Raghavachari, K.; Al-Laham, M. A.; Zakrzewski, V. G.; Ortiz, J. V.; Foresman, J. B.; Cioslowski, J.; Stefanov, B. B.; Nanayakkara, A.; Challacombe, M.; Peng, C. Y.; Ayala, P. Y.; Chen, W.; Wong, M. W.; Andres, J. L.; Replogle, E. L.; Gomperts, R.; Martin, R. L.; Fox, D. L.; Binkley, J. S.; Defrees, D. J.; Baker, J.; Stewart, J. P.; Head-Gorden, M.; Gonzalez, C.; Pople, J. A. *Gaussian 94*; Gaussian Inc.: Pittsburgh, PA, 1995.

(24) Petersson, G. A.; Bennett, A.; Tensfeldt, T. G.; Al-Laham, M. A.; Shirley, W. A.; Mantzauis, J. *J. Chem. Phys.* **1988**, *89*, 2193−2218.

Table 1. Peak Positions (in cm^{-1}) and Assignments of the Normal Raman (OR) Spectrum of BDMT and SER Spectra of BDMT on Gold and Silver (The Scaled[a] 6-31G* Frequencies (in cm^{-1}) Are Also Given)

				6-31G* frequencies			
BDMT solid OR	BDMT/Au SER	BDMT/Ag SER	assignment	neu[b]	dian[c]	sym[d]	Wilson's notation
3056	3052	3050 (vw)	νCH(arom)	3053	3051	A′	2
3035				3015	3050	A′	13
3010					2961	A′	7_b
2928	2924	2916 (w)	νCH(CH_2)asym	2957	2838	A″	
				2956	2837	A″	
2840			νCH(CH_2)sym	2918	2827	A′	
				2917	2826	A′	
2553	2562		νSH	2626		A′	
				2625		A′	
1611	1609	1609	νcc(ring stret)	1644	1628	A′	8_a, 8_b
1576			νcc(ring stret)	1592	1576	A′	
1430			CH_2 deform.	1467	1461	A′	
1254	1253 (sh)		CH_2 wagging	1339		A′	
	1224	1224	CH_2 wagging	1290	1309	A′	
					1238	A′	
1200	1201	1201	sub.-sen. band	1195	1184	A″	
				1184	1181	A″	
				1170	1164	A′	
1183	1181	1177	β_{C-H}	984	986	A″	9_a, 9_b
978			γ_{C-H}	941	902	A″	18_a
838	838	842	γ_{C-H}	894	861	A″	10_a, 10_b
792	785		δ_{CSH}	850	857	A″	
743	743	743	γ_{C-H}	818	811	A′	11
676	668	662	ν_{C-S}	731	738	A′	
638	636	634	ν_{C-S}	694	692	A″	
				625	626	A′	
	515	500		496	517	A′	20_a
344	355	345	sub.-sen. band[e]	326	318	A″	6_a
	296	233	metal S vibn				
			CH_2 deform.	286	279	A″	
			CS bend	164	167	A′	
				161		A″	

[a] Multiplied by 0.9. [b] Neutral molecule. [c] Thiolate dianion in the singlet state, frequencies of the triplet state were similar. [d] Symmetry notation. [e] Substituent-sensitive band. γ-Out-of-plane vibration, β-in-plane vibration, δ-bending vibration.

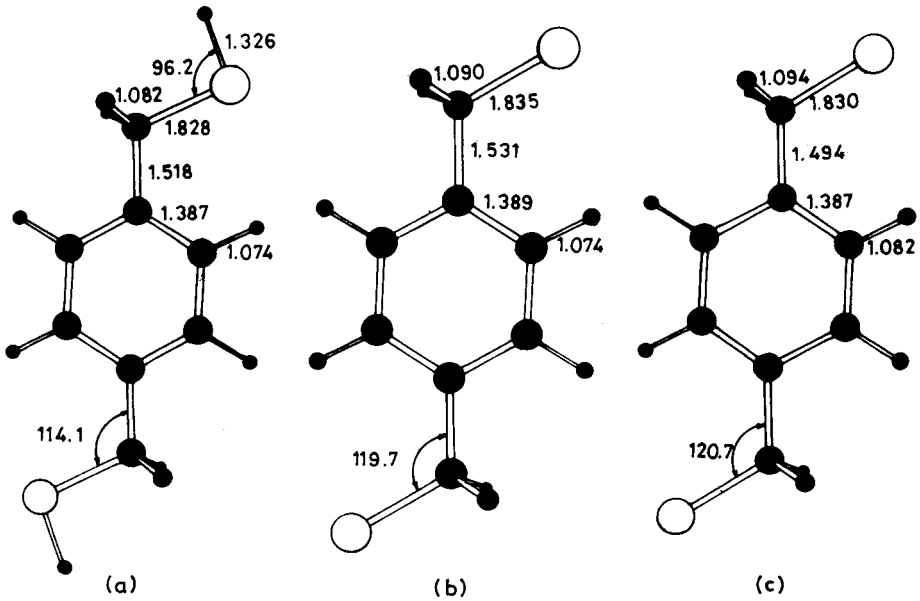

Figure 2. HF/6-31G* optimized structures of (a) neutral BDMT and the thiolate dianion in the (b) singlet and (c) triplet states. Important molecular parameters are indicated.

Ag.[6c] The interaction on Ag leads to the loss of both the thiol protons; therefore, the adsorption geometries in both cases are different. The complete loss of the S−H stretch on Ag is a clear indication that the SERS spectrum is arising only from the monolayers.

Prominent among the differences between the two cases are the almost complete disappearance of the aromatic C−H vibrations (ν_2) in the silver spectrum and the presence of certain additional features in the gold spectrum. The absence of the ν_2 mode in the case of the silver monolayer provides direct evidence to the flat orientation of the benzene ring, as has been suggested by Gao and Weaver[6e] and Kim et al.[6q] In addition, adsorption also results in frequency downshifts of the ring modes. The shifts are substantially smaller than those observed for benzene and substituted benzenes adsorbed on silver[6b,h,q] where π-interaction, whether donation from the π-orbital of the ring to the silver orbitals or the reverse donation

to π^* of benzene occurs. Therefore, it can be concluded that the adsorption does not result in significant π-interaction. The π-interaction between the ring and the surface leads to frequency shifts of the order of 10 cm^{-1} for most of the bands[6a] such as ν_8. In this case, the shift is only marginal, of the order of 3 cm^{-1}. However, the C−S stretch downshifts substantially. Whereas all the bands are downshifted upon adsorption, the S−H stretching is upshifted by as much as 9 cm^{-1} in the monolayer. This may be taken as an indication of the absence of intermolecular hydrogen bonding involving the thiol protons in the monolayer. The monolayer packing density will be smaller than that of the solid and consequently intermolecular distance will be larger. Assuming a $(\sqrt{3} \times \sqrt{3})R\ 30°$ adlayer of sulfur, the nearest neighbor distance is about 5 Å, and intermolecular hydrogen bonding will be weaker than that in the solid state. In addition to the shifts observed, adsorption also leads to the broadening of most of the bands, which also supports chemisorption. Another important aspect to note is that the frequency shifts are larger for Ag than for Au. This is particularly evident in the νC−H of CH_2 and νC−S (see Table 1). This shows that the interaction is stronger in Ag than in Au.

The almost complete loss of ν_2 is understandable from the published SERS selection rules.[3,6] If the benzene ring is flat on the surface, the molecular and surface plains are collinear and the component of the polarizability tensor normal to the surface for ν_2 will be very small. The polarizability tensor for these vibrations lie almost along the bond axis. This issue has been discussed in several recent publications, especially from the groups of Weaver, Kim, and Pemberton.[5,6a,d] The surface-selection rule suggests that the surface enhancement of this mode will be poor for the flat geometry.

The CH_2 wagging region (1200−1300 cm^{-1}) shows a substantial difference for the two surfaces. The peak at 1218 cm^{-1} in the Ag monolayer can be correlated to this mode, which is downshifted as reported before.[6q] The two CH_2's are the same in the case of silver, but for Au it is not the case. As a result, one CH_2 wagging is shifted only marginally in the case of Au, which appears at 1253 cm^{-1}, and in Ag this peak is absent. Further evidence to this assignment comes from the pH-dependent measurements. Upon exposure of the monolayer to a solution of NaOH, the peak at 1253 cm^{-1} completely disappears (Figure 1d). At the same time, the S−H stretching disappears, suggesting the formation of $BDMT^{2-}$. In this case, the CH_2 wagging region is similar to that of Ag. Confirmatory evidence for the formation of $BDMT^{2-}$ is seen in the complete disappearance of the C−S−H bending mode at 785 cm^{-1} in the Au monolayer exposed to NaOH solution. It may be seen that the Ag monolayer does not show this feature at all and it is present in the bare Au monolayer.

The C−S stretching region in both cases manifests similar features, suggesting similar interaction in both cases. In Au, however, a shoulder at 676 cm^{-1} is evident, corresponding to the C−S stretching of the free thiol. This frequency is the same as in the OR spectrum of BDMT. Along with this, the C−S−H bending at 785 cm^{-1} is also evident, lending support to the proposed adsorbate geometry. These two features change substantially upon exposure of the monolayer to a solution of NaOH (Figure 1d). While the latter disappears completely, the former shifts to a lower value and merges with the C−S stretch at 636 cm^{-1}.

Taken together, it can be concluded that BDMT adsorbs head-on on Au with the phenyl ring lying perpendicular to the surface. One thiol group is poking up at the surface of the monolayer. The chemistry of this thiol group will be discussed in a later section. On silver, the chemisorption leads to the loss of two thiol protons and the phenyl ring lies flat on the surface. Additional support to the adsorption geometry comes from the C−C−C ring deformation mode ν_8, preferential enhancement of which is much smaller in Ag. Compare, for example, the intensities of bands at 1609 cm^{-1}(ν_8) and 1218 cm^{-1} (CH_2 wagg) for the Ag and Au monolayers. The ν_8 mode is predominantly parallel to the ring and therefore is much stronger if the ring lies perpendicular to the surface, although the preferential enhancement of modes of this kind is still not fully resolved in the literature.[6a] CH_2 wagg will not be affected whether the ring lies flat or perpendicular to the surface. The loss of ν_8 intensity in Ag then suggests that the ring lies flat in this case. Although the ring lies flat, this does not enhance π-interaction. Had there been significant π-interaction, the magnitude of it would be different in both cases, leading to differences in the ring modes. But we find that ν_8 occurs at the same frequency in both cases. Differences observed are, however, in the modes closer to the sulfur atoms, such as those due to C−H and C−S.

Having established qualitatively the surface geometry of the adsorbates, it may be interesting to inquire why this difference should occur. From a large number of studies, it has been established that on Au(111) the strongest binding location is the 3-fold hollow site. The evaporated films will be mostly (111) as has been shown earlier.[25] In $BDMT^{2-}$, the S−S distance is about 8.4 Å (from calculations, see Figure 2), comparable to one of the near-neighbor hollow-site distances (8.4 Å) in Ag(111) (8.343 Å) and Au(111) (8.328 Å). This calculation assumes an atomic diameter of 2.890 Å for Ag and 2.885 Å for Au. There are also on top and hollow sites separated at the same distance. Thus, the difference in adsorption geometry does not seem to be due to a difference in the availability of proper adsorption sites. The only possibility we can think of is the difference in π-interaction. As the data suggest, even though the interaction is weak, it is greater in Ag. In Au, however, the adsorption geometry leads to larger packing density and the forces of self-assembly compensate for the additional π-interaction. In fact, it appears that a more complete self-assembly leads to a monolayer which is thermally more stable (see below).

To adsorb with the molecular plane collinear to the surface and to keep the geometry similar to that of the free molecule, the orbitals of sulfur interacting with the surface have to be perpendicular to the molecular plane and such a geometry is shown in Figure 3a. This flat orientation could bring the phenyl π-orbitals in close proximity to the surface, leading to shift in the ring vibrations, but due to the presence of CH_2 groups, the benzene ring is maintained at a larger distance from the surface. It may be noted that the Ag−S distance is 1.92 Å whereas it is 2.01 Å in Au.[10] Taking a distance of 2.82 Å between the benzene ring and the sulfur atoms (Figure 2), the approximate distance between the surface and ring works to be 4.74 Å for Ag. This large distance is the principal reason for the weak π-interaction. For a similar geometry, the distance would have been larger for Au, leading to a still weaker π-interaction. A different orbital interaction could lead to a structure depicted in Figure 3b in the case of Au. In this structure, lateral van der Waals interaction is strong, leading to an organized monolayer, and the energetics prefer this to the face-on structure. An additional aspect which could contribute to the difference

(25) Chidsey, C. E. D.; Loiacono, D. N.; Sleator, T.; Nakahara, S. *Surf. Sci.* **1988**, *200*, 45−66.

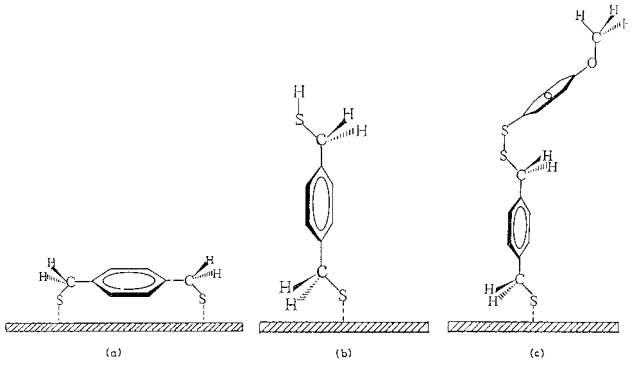

Figure 3. Proposed structures of BDMT monolayers on (a) Ag, (b) Au, and (c) MOBT monolayer on BDMT. Note that the adsorbate geometry is only schematic.

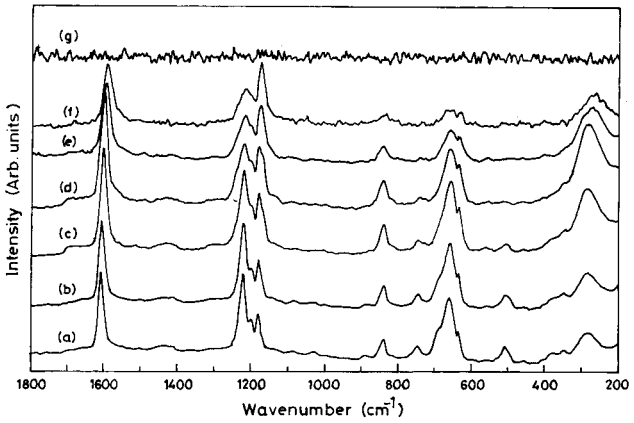

Figure 4. Temperature-dependent SER spectra of the BDMT monolayer exposed to NaOH solution. The temperatures are (a) 298 K, (b) 323 K, (c) 373 K, (d) 398 K, (e) 423 K, (f) 448 K, and (g) 493 K.

in adsorption geometries is the difference in S−H deprotonation kinetics on the two surfaces.

Stability and Dynamics. The monolayers are stable up to a temperature of 423 K. They also retain the properties even after several weeks of their preparation. We did not observe noticeable changes in the spectral features upon exposure to laboratory atmosphere for a couple of months. The monolayers appear to retain the properties after immersion in water and ethanol. No decrease in the SERS intensity was seen in the alcohol- or water-exposed samples. To investigate the thermal stability of the monolayer in detail, we measured their temperature-dependent Raman spectra. The data from the Au monolayer exposed to NaOH solution in the 1800−200-cm^{-1} region are shown in Figure 4. The spectral features are the same at all the temperature ranges investigated; however, certain shifts and intensity changes are seen. At all temperatures, the C−S region is the same, indicating the integrity of the monolayer and any absence of change in the adsorption site. Note the absence of the CH_2 wagging at 1253 cm^{-1} and the C−S−H bending mode at 785 cm^{-1} (upon exposure to NaOH solution) as discussed before. Thermal broadening occurs for all the bands (note particularly the ν_8 band at 1609 cm^{-1}, which shows substantial broadening) and the monolayer begins to desorb at 423 K, at a much higher temperature than alkanethiol SAMs.[22] At 423 K, certain new bands begin to appear, suggesting changes in the monolayer structure. Beyond 473 K, spectral features are completely changed. Upon cooling, the spectrum does not show the reappearance of any features, suggesting the absence of adventitious species.

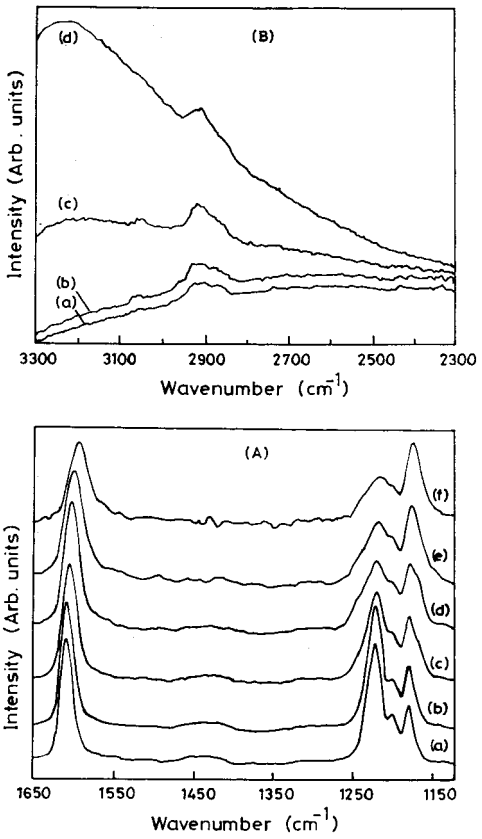

Figure 5. Spectra as in Figure 4 in the (A) low- and (B) high-frequency regions. Note the downshift of the 1600-cm^{-1} band and the intensity reversal in the CH_2 wagging region. The temperatures are (a) 298 K, (b) 323 K, (c) 373 K, (d) 398 K, (e) 423 K, and (f) 448 K. The top figure shows the corresponding spectra in the C−H region. The temperatures are (a) 298 K, (b) 323 K, (c) 373 K, and (d) 398 K. Beyond 398 K, the blackbody radiation masked the features.

Looking at the changes in more detail (Figure 5), we see that the band at 1609 cm^{-1} undergoes significant downshift beginning at 373 K. Around this temperature, the substituent CH_2 wagging mode begins to lose intensity and a shoulder at 1250 cm^{-1} starts appearing, although no frequency shift is observed (Figure 5). While these changes are happening, the aromatic C−H stretching mode decreases in intensity (Figure 5). Beyond 125 °C, the C−H region is not observable due to high blackbody radiation from the sample.[26] These changes suggest that the BDMT dianion begins to fall flat at the surface as the temperature is increased, leading to a downshift of ν_8 due to increased π-interaction with the surface. This leads to the partial disappearance of the aromatic C−H stretching mode since the mode lies along the molecular plane. While this change is occurring, the substituent CH_2's become different, which manifests in the spectrum as a shoulder in the CH_2 wagging region.

To confirm these changes, we looked at the temperature dependence of the pure BDMT monolayer itself. There is a possibility that in the NaOH-exposed monolayer, the motion of the benzene ring is driven by the presence of the $-CH_2-S^-$ moiety at the surface, which looks for a binding site. Therefore, it is important to see the origin of the dynamics. The data presented in Figure 6 show that the temperature dependence is similar for the bare BDMT monolayer as well. The important difference is that the

(26) Schrader, B.; Hoffmann, A.; Keller, S. *Spectochim. Acta* **1991**, *47A*, 1135.

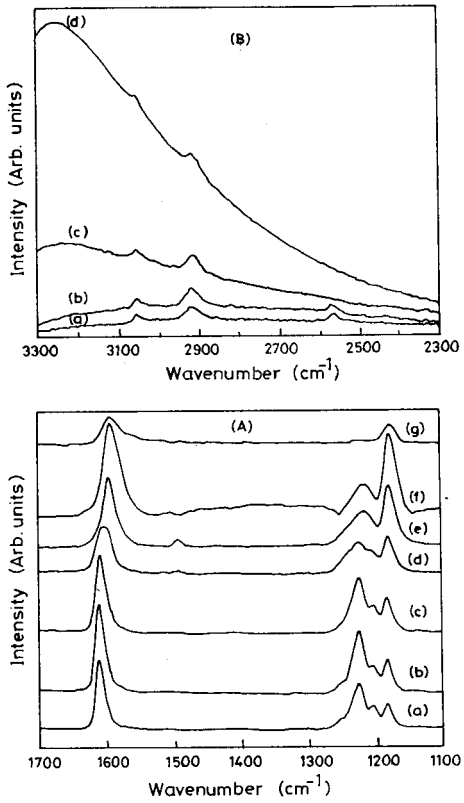

Figure 6. Temperature-dependent SER spectra of the bare BDMT monolayer on Au in (A) low- and (B) high-frequency regions. Only part of the spectrum is shown for clarity. The temperatures are (a) 298 K, (b) 323 K, (c) 373 K, (d) 398 K, (e) 423 K, (f) 448 K, and (g) 473 K. B shows spectra up to 398 K.

dynamics can be monitored with the S−H stretch also. It disappears much before the changes in the region of CH_2 deformation bands where the emergence of an additional structure occurs at 398 K. The loss of S−H also leads to the disappearance of the C−S−H bend at 785 cm^{-1} (not shown). Simultaneously, the band at 1600 cm^{-1} undergoes a downshift, indicating the presence of another adsorbate geometry. At 398 K, both these adsorbed forms are observable and the band gets broadened. The movement of the monolayer is also manifested in the appearance of a new band at 1475 cm^{-1} in the in-between temperatures. This mode assigned to a CH_2 deformation becomes Raman-active during the structural transformation. Taken together, the data conclusively establish the changes in adsorption geometry with temperature.

While the S−H stretch disappears, the aromatic C−H is still observable. It tends to suggest that the molecular plane is not completely parallel to the surface (see below). Similar dynamics of NaOH exposed and bare BDMT monolayers suggest that surface binding can occur from the thiol or from the thiolate species.

In Ag, one would have expected a higher desorption temperature due to the flat orientation of the benzene ring (possible presence of π-interaction), but the lack of it indicates that such an interaction is minimal. The Ag data are shown in Figure 7. Only gradual change in intensity of all the bands are seen; no intensity reversal or shift in band position is seen. The data can be interpreted in terms of direct desorption of the adsorbate from the surface. It is interesting to see that the mobility of molecules and concomitant dynamics is seen only in the case of the Au monolayer. This also supports the above-discussed adsorbate geometry. In the proposed structure on silver, there is no possibility of drastic changes

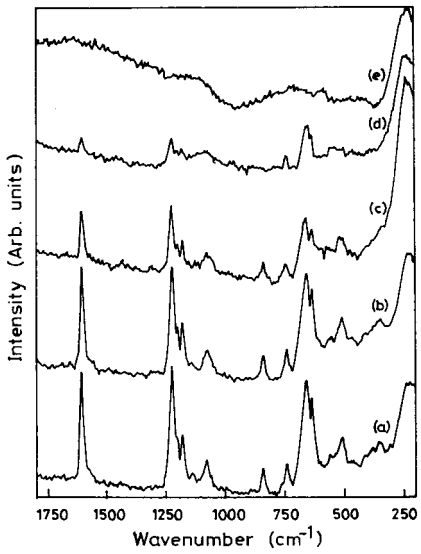

Figure 7. Temperature-dependent SER spectra of the BDMT monolayer on Ag. The temperatures are (a) 298 K, (b) 323 K, (c) 373 K, (d) 423 K, and (e) 473 K.

in the adsorbate geometry, leading to the absence of any observable changes in the temperature-dependent Raman spectrum. The significant difference in desorption temperatures of these two monolayers point to the importance of energetics of lateral interaction. In a π-system of this kind, lateral interaction present in the case of an Au monolayer more than offsets the additional enthalpy of metal−S interaction present in the Ag monolayer.

One might argue that the falling down of the BDMT monolayer on Au is contrary to entropic considerations. It needs to be remembered that the falling down does not lead to appreciable π-interaction between the ring and the surface. We do not see evidence for the complete disappearance of aromatic C−H stretching modes. This suggests that there is significant orientational freedom in the flat geometry. The monolayer to begin with should be well-ordered as manifested from the high desorption temperature compared to that on Ag. Therefore, in a qualitative sense, falling down need not be an entropy downhill process.

One important point to be addressed is that concerning the sequences of events leading to the "falling down" process upon an increase in temperature. It is likely that the binding site of sulfur in the BDMT monolayer is similar to that of alkanethiols where all the available 3-fold hollow sites are not occupied by sulfur. For a molecule of the dimension of BDMT, the near-neighbor sulfur distance is not substantially smaller than molecular dimensions. Therefore, regardless of the orientation of the molecules, the surface coverage may not be greatly different. Also, all the molecules need not fall down along one direction only. Thus, falling down may not cause desorption of some molecules. There is no intensity change in the spectra to suggest such a loss. Also, note that the aromatic C−H stretching mode is not completely lost upon falling down, which indicates that the molecular plane is not perfectly flat. Another aspect to keep in mind is the likelihood of molecular motions among adsorption sites which would be facilitated at high temperatures. Both of these aspects might be responsible for the observed changes.

Reactivity. To investigate the reactivity of the monolayers, certain experiments were performed. A monolayer prepared on Au upon exposure to NaOH solution loses the thiol proton. The SERS spectrum in the C−H region of the exposed monolayer is shown in Figure 1, showing

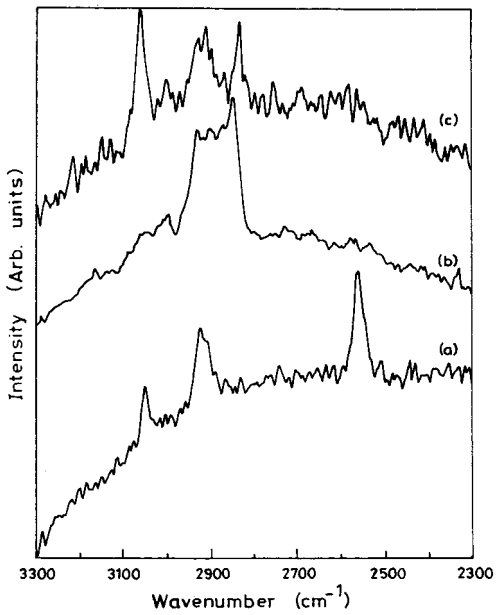

Figure 8. C−H stretching region of the (a) free BDMT monolayer and (c) that upon exposure to MOBT. The corresponding region of MOBT monolayer on Au is shown in (b).

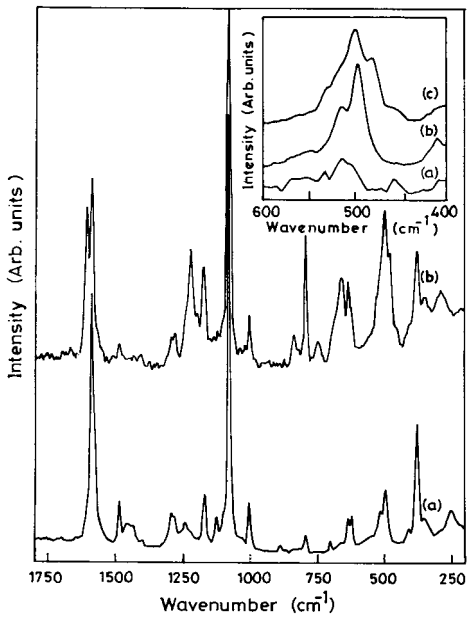

Figure 9. Low-frequency region of monolayers of (a) MOBT and (b) BDMT on Au exposed to MOBT. Inset shows the S−S stretching region of (a) BDMT, (b) MOBT, and (c) MOBT-exposed BDMT monolayers. Note the new peak at 480 cm^{-1} in (c).

the complete absence of the thiol proton. However, the orientation of the phenyl ring has not changed as indicated by the presence of the aromatic C−H bands just as that in the bare monolayer. The low-frequency region shows only marginal changes, which has been discussed before. In the case of the Ag monolayer, NaOH exposure does not result in any change at all.

Having established that the thiol proton can be exchanged without affecting the self-assembly, we tried to modify the monolayer by exposing it to 4-methoxybenzenethiol (MOBT). The first noticeable change is the absence of the S−H stretching frequency in the MOBT-exposed BDMT monolayer (Figure 8c). However, C−H frequencies of MOBT (Figure 8b) are seen in addition to those of BDMT (Figure 8a). It is also important to note that the aromatic ring C−H vibrations are present in the exposed monolayer. A few additional features appear in the low-frequency region which can be seen in Figure 9. These features can be attributed to the reaction of MOBT with BDMT. The spectrum can be represented as a sum of the spectra of BDMT and MOBT on Au except in the 700−400-cm^{-1} region. In the C−S region, the exposure does not result in changes attributable to MOBT chemisorption on Au. To confirm this, we carried out the adsorption of MOBT directly on a clean Au film; the spectrum of the MOBT monolayer is also given in Figure 9 (see also in Figure 8). MOBT adsorption[27] on Au results in C−S stretches at 636 and 620 cm^{-1}. In MOBT liquid, these bands were at 637 and 625 cm^{-1}, respectively. The downshift of one of the bands indicates that this is the one sensitive to adsorption. The 620-cm^{-1} band in the pure MOBT monolayer appears as a shoulder at 625 cm^{-1} in Figure 9b, which suggests that MOBT does not chemisorb at the surface directly. The other band occurs at 636 cm^{-1} itself in the mixed monolayer. The absence of significant changes in the C−S bands is evidence for the absence of direct chemisorption at the surface. Moreover, if MOBT has to chemisorb at the surface, some of the BDMT molecules have to desorb, leading to a decrease in the intensity of the BDMT bands which is not observed. On the contrary, the absolute intensities of the bands remain almost the same as those in the bare BDMT monolayer. Looking at the region of ν_8, it appears that the relative ratio of BDMT and MOBT at the surface is roughly 1:1.

The foregoing suggests reaction between MOBT and BDMT, leading to an organic bilayer. The possible reaction between the two molecules to manifest the kind of spectral changes is the disulfide formation. The S−S stretching frequency in disulfides of this kind (ϕ−C−S−S−C−ϕ, where ϕ represents an aromatic system) should occur[28] in the range of 470−500 cm^{-1}. An examination of this range shows a prominent feature at 480 cm^{-1}, which is completely new (see the inset of Figure 9) which we attribute to the S−S stretching vibration. This is the only characteristic new feature of high intensity in the spectrum of the exposed monolayer. There can be a few other associated features; we do not see them distinctly, probably because of the overlapping bands.

The reaction between thiols to form disulfide is, although possible in solution, not observed when BDMT and MOBT are mixed in solution at room temperature. The fact that this occurs at the monolayer surface indicates the possibility of similar reactions with other thiols. This could be a novel method of making organic multilayers with specific functionalities. The simplicity of the method—as simple as the formation of SAMs—would make it possible to extend the SAM chemistry further. In our opinion, this new reaction is presumably due to the preferred arrangement of reactants at the monolayer surface. Confirmatory evidence for this is provided by the complete absence of such features in the case of the Ag monolayer. The fact that no S−H stretch is observable implies that all the thiol groups have undergone the transformation. This implies a bilayer with a high degree of order, an improvement over the earlier methods of forming multilayer,[21] suggesting the need for specific chemical reactions in multilayer formation. It is clear from the data that BDMT itself does not cause bilayer formation,

(27) Venkataramanan, M.; Murty, K. V. G. K.; Pradeep, T., to be published.

(28) Freeman, S. K. *Application of Laser Raman Spectroscopy*; Wiley-Interscience: NewYork, 1974; p 225.

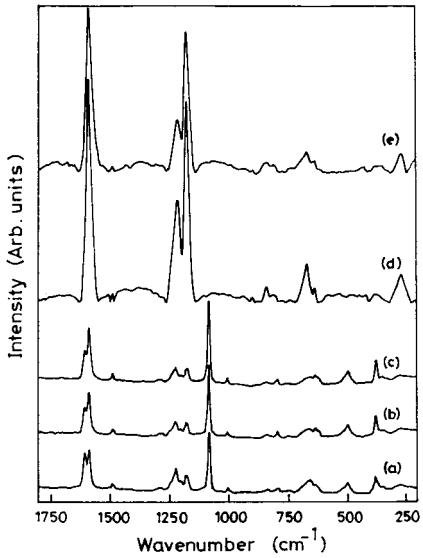

Figure 10. Temperature-dependent SER spectra of MOBT-exposed BDMT monolayer. The temperatures are (a) 298 K, (b) 323 K, (c) 423 K, (d) 448 K, and (e) 473 K. Note the disappearance of MOBT features after 423 K.

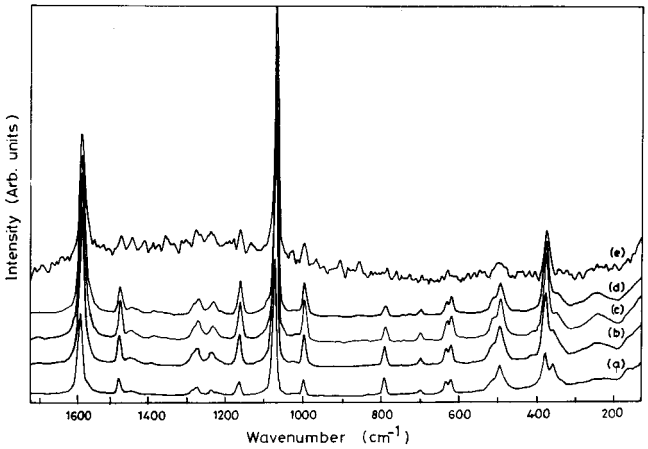

Figure 11. Temperature-dependent SER spectra of MOBT monolayers on Au. The temperatures are (a) 298 K, (b) 323 K, (c) 373 K, (d) 423 K, and (e) 473 K. Note the presence of features even up to 473 K.

pointing to the importance of chemical affinity between the interacting molecules in the observed process (see below).

To compare the stability of the reacted monolayers, temperature-dependent measurements of the reacted monolayers were performed. The temperature dependence of the Raman spectrum of the BDMT−MOBT monolayer is shown in Figure 10. It is apparent that at a temperature of 448 K, the MOBT part disappears. The desorption is evident by the absence of the peaks at 1600 and 1075 cm^{-1}. This is the temperature at which the disulfide peak at 480 cm^{-1} also disappears. After the desorption, the spectrum appears similar to that of the BDMT monolayer at the corresponding temperature. Subsequent heating leads to the desorption of BDMT as well. To compare the results, temperature dependence of the pure MOBT monolayer was also investigated (Figure 11). The behavior was found to be substantially different from that of the mixed monolayer. The monolayer is stable up to to a temperature of 423 K, and even at 473 K, the features are visible. The monolayer does not exhibit any dynamics upon heating.

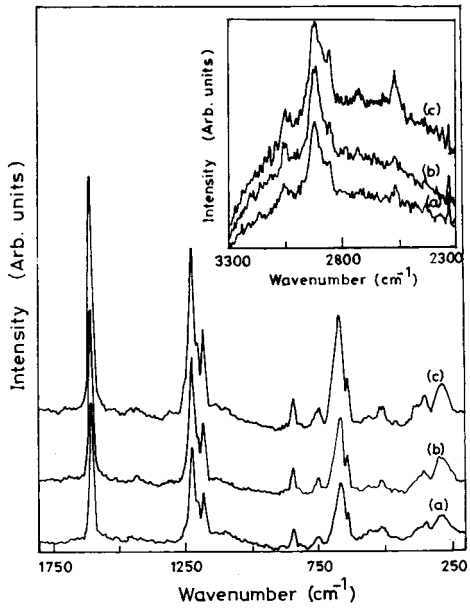

Figure 12. SER spectra of alkanethiol exposed BDMT monolayers on Au: (a) Propanethiol, (b) Octanethiol and (c) Octadecanethiol. Inset shows the C−H stretching region of all.

The prototypical bilayer is schematically represented in Figure 3c. The stereochemistry implied in the figure is only tentative and needs confirmatory evidence. To investigate the reactions further, alkanethiols were also exposed to the BDMT monolayer on Au. Spectra of the monolayers upon exposure to propane, octane, and octadecane thiols are shown in Figure 12. In all the spectra, the peak due to the S−H stretch decreases in intensity as a result of exposure to the thiol (see the inset). Drastic decrease is seen in the case of shorter alkane chain thiols. Peaks attributable to the constituents are seen in the spectra, although the alkane peaks are much weaker in intensity which is the case in bare alkanethiol SAMs[22] as well (the sensitivity for aromatic systems is better in Raman). Physisorption of alkanethiols on the BDMT monolayer would not have resulted in the loss of an S−H proton. Therefore, we suggest that reaction has occurred in these cases as well, although we do not see any clear evidence for a S−S bond. However, there are certain changes in the 500-cm^{-1} region of all the spectra which may be attributed to a weak S−S feature masked by the ring modes.

XPS Studies and X-ray-Induced Damage of the Monolayers. The monolayers were subjected to XPS investigations, with particular emphasis to the S 2p region. Normal alkanethiols manifest a peak at 162 eV in this part of the spectrum, corresponding to the thiolate (RS^-) species.[13,29] It has been shown that the type of bonding is the same in a series of similar *n*-alkanethiol monolayers and the S 2p shows a peak at the same position, although the inelastic background of the peak increases with thickness as expected.[30] The Mg Kα induced XPS of the BDMT monolayers in the S2p region is shown in Figure 13. The spectrum (Figure 13a) corresponds to three distinctly different sulfurs. The spectrum is similar to the spectrum of the dithiol monolayer on gold studied by Colvin et al.[31] Although the thiol and thiolate are expected to manifest as two separate peaks, they are expected in

(29) (a) Bain, C. D.; Troughton, E. B.; Tao, Y.-T.; Evall, J.; Whitesides, G. M.; Nuzzo, R. G. *J. Am. Chem. Soc.* **1989**, *111*, 321−335. (b) Laibinis, P. E.; Whitesides, G. M.; Allara, D. L.; Tao, Y.-T.; Parikh, A. N.; Nuzzo, R. G. *J. Am. Chem. Soc.* **1991**, *113*, 7152−7167.

(30) Bindu, V.; Pradeep, T. *Vacuum* **1998**, *49*, 63−66.

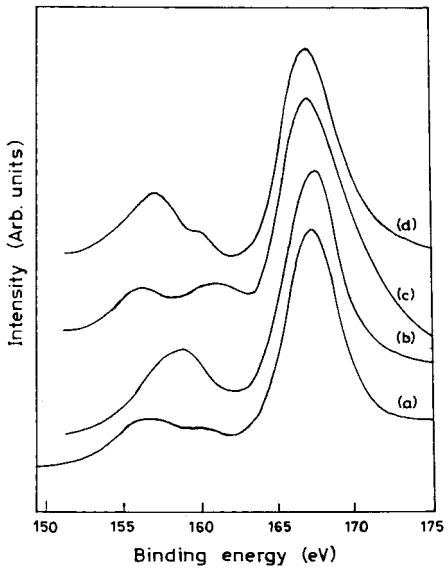

Figure 13. S(2p) X-ray photoelectron spectra of BDMT monolayers on (a) Au and (b) Ag, (c) MOBT monolayer on Au, and (d) MOBT-exposed BDMT monolayer on Au. Note the presence of the peak at ~160 eV in the BDMT monolayers on Au.

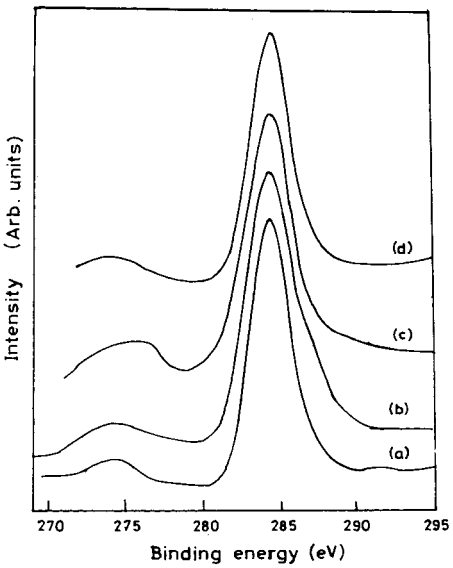

Figure 14. C(1s) region of the BDMT monolayers on (a) Au and (b) Ag, (c) MOBT monolayer on Au, and (d) MOBT-exposed BDMT monolayer on Au. The low BE feature separated by 10 eV from the main peak is due to Mg $K\alpha_{3,4}$ radiation.

the range of 162−164 eV of binding energy. The substantial shift in the binding energies are explained as due to beam-induced damage of the thiol surface.[31] This effect is particularly important considering the fact that the monolayer thickness is small. We interpret the peak at 168.5 eV as due to sulfate or sulfite which formed as a result of reaction between the X-ray excited monolayer and residual gases in the vacuum chamber which are principally H_2O and CO. This is reasonable since the vacuum was of the order of 5×10^{-8} Torr and the measurement times were of the order of 40 min for each spectrum owing to the poor signal quality. In addition to this exposure, the sample was also exposed to X-rays during the general survey scan, prior to the S 2p measurement. The low binding energy sulfur at 158 eV

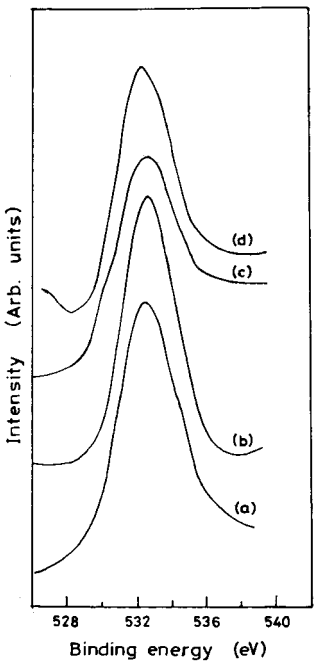

Figure 15. O(1s) X-ray photoelectron spectra of the BDMT monolayers on (a) Au and (b) Ag, (c) MOBT monolayer on Au, and (d) MOBT-exposed BDMT monolayer on Au.

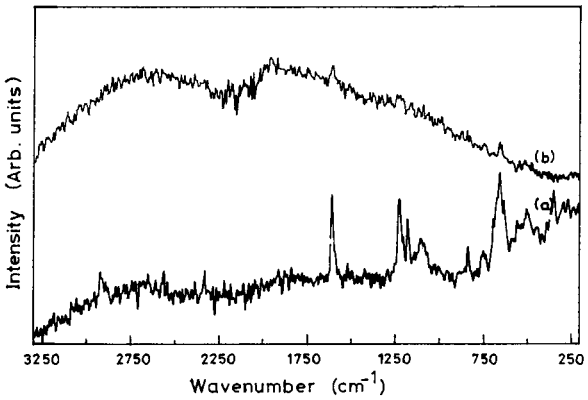

Figure 16. The SER spectra of the BDMT monolayers on (a) Au and (b) Ag after X-ray irradiation. Note the almost complete disappearance of BDMT features in the Ag case. Comparison of (a) with Figure 1b shows that new peaks have appeared after X-ray exposure.

corresponds to a more reduced form than the thiolate. Both of these peaks are seen in the SAM of hexanedithiol on gold as well.[31] In addition, we attribute the shoulder at 162 eV to the thiolate sulfur, which has not undergone beam-induced damage. This binding energy is characteristic of the alkanethiolate structure. The observation of the thiolate sulfur indicates that some of the monolayer is still preserved even after X-ray exposure. This is in conformity with the SERS measurements of the exposed films (see below). Short-chain-length SAMs such as that of naphthalenedisulfide is also shown to exhibit X-ray-induced damage.[33]

The XPS spectrum of the monolayer on silver (Figure 13b) shows similar features, but the thiolate structure is not clearly manifested. The spectrum is composed of two peaks, at 158 and 168 eV, and the explanation is the same

(31) Colvin, V. L.; Goldstein, A. N.; Alivisatos, A. P. *J. Am. Chem. Soc.* **1992**, *114*, 5221−5230.

(32) Briggis, D.; Seah, M. P. *Practical Surface Analysis*: John Wiley and Sons: New York, 1983.

(33) Bandyopadhyay, K.; Sastry, M.; Paul, V.; Vijayamohanan, K. *Langmuir*, in press.

as above. The thiolate peak at 162 eV is not manifested, indicating that the monolayer is more susceptible for damage which is in accordance with the proposed structure. Conformatory evidence is seen in the SER spectrum of the exposed monolayer (see below).

The spectra of the MOBT monolayer (Figure 13c) and the prototypical bilayer on Au (Figure 13d) are also similar to that of BDMT. In all the cases, the three-peak structure is evident and the interpretation is the same. It is noted that the ratio of the intensities of the low binding energy (BE) and the high BE peaks is substantially greater in the bilayer.

The C 1s in all cases (Figure 14) appears as a single symmetric peak at 285 eV of BE as expected. The beam-induced effects are not manifested in it, suggesting that it is confined to the sulfur. The C 1s spectra of all the monolayers are presented in Figure 13. The presence of damage is manifested in the O 1s spectra also. In the BDMT monolayer on Au we expect no oxygen just as in the case of alkanethiol SAMs. But as a result of X-ray-induced damage O 1s peaks are observed as shown in Figure 15. O 1s appears as a single peak in the BDMT monolayers on Au and Ag. In the BDMT and BDMT/MOBT monolayers a high BE shoulder is also observable. We attribute this to the integral monolayer itself. The low BE structures are attributable to sulfate or sulfite. The intensity of which increases with X-ray exposure and saturates after 30 min of exposure.

The X-ray-induced damage of the films was confirmed by SERS measurements of the films after X-ray exposure (Figure 16). Whereas the Au film shows only some changes from the parent film (Figure 1), the silver film shows complete degradation. In the case of Au, the features corresponding to BDMT are apparent; however, the spectrum also shows new peaks. Although a complete analysis is not attempted, chemical changes are indeed apparent. In the case of Ag, the BDMT features are barely observable. Complete damage of the monolayer can be inferred. The results support XPS data. In Au, where the XPS spectrum shows a peak at 162 eV (corresponding to the thiolate structure), whereas that is completely absent in the silver spectrum. It can be concluded that, in Au, some of the BDMT monolayer is still present, whereas in Ag, it is completely damaged.

Conclusions

The study shows that BDMT adsorbs dissociatively on Au and Ag surfaces. On Ag both the thiolate protons are lost upon adsorption and on Au only one is lost. As a consequence of this difference in adsorption geometries, the molecule lies flat on the Ag surface whereas it is perpendicular to the surface on Au. Although there is significant difference in the adsorbate geometry, there is very little π-interaction between the ring and the surface, leading to only small frequency shifts upon adsorption. The BDMT monolayers are more stable thermally than alkanethiol self-assembled monolayers and begin to desorb around 423 K as an integral unit. In the case of Au, the desorption occurs with significant associated dynamics, whereas it is eventless on Ag. It is surprising that the monolayer on Ag desorbs at a lower temperature than that on Au. For a flat geometry one would expect more π-interaction and consequently stronger adsorption. However, the desorption occurs at a lower temperature. This implies the importance of self-assembly in the energetics of desorption. A flat geometry will not permit larger surface coverage, whereas in a head-on configuration the coverage is more. This higher packing density and consequent lateral interaction between the molecules seems to be the reason for the higher desorption temperature on Au. The BDMT monolayer on Au loses its available thiol proton upon exposure to alkaline solutions. The thiol group at the surface reacts with incoming thiols such as MOBT, leading to the formation of disulfides. This reaction is suggested as a prototypical organic bilayer formation with wide application in chemistry. The Ag surface does not show a corresponding reaction. Alkanethiols show similar reactions, although the S−S bond is not conclusively established. The XPS studies suggest the importance of beam-induced damage in these films and leaves a cautionary note on the analysis of dithiol monolayers.

Acknowledgment. T.P acknowledges financial support from the Department of Science and Technology, Government of India, the Jawaharlal Nehru Centre for Advanced Scientific Research, and the Rajiv Gandhi Foundation.

LA980249I